Supporting information

Optics determines the electrochemiluminescence signal of bead-based immunoassays

Dongni Han,[a,b] Dechen Jiang,[c] Giovanni Valenti,[d] Francesco Paolucci,[d] Frédéric Kanoufi,[e] Patrick Chaumet,[f] Danjun Fang,*,[b] Neso Sojic*,[a]

[a] *Univ. Bordeaux, CNRS, Bordeaux INP, ISM, UMR 5255, ENSCBP, 33607, Pessac, France*

[b] *School of Pharmacy, Nanjing Medical University, Nanjing, Jiangsu, 211126, China*

[c] *State Key Laboratory of Analytical Chemistry for Life Science and School of Chemistry and Chemical Engineering, Nanjing University, Nanjing, Jiangsu, 210023, China*

[d] *Department of Chemistry "G. Ciamician", University of Bologna, Via Selmi 2, 40126, Bologna, Italy*

[e] *Université Paris Cité, ITODYS, CNRS, F-75013 Paris, France*

[f] *Institut Fresnel, Aix Marseille Univ, CNRS, Centrale Marseille, 13013, Marseille, France*

Emails: sojic@u-bordeaux.fr; djf@njmu.edu.cn

Table of Contents

1. Experimental PL and ECL lateral views

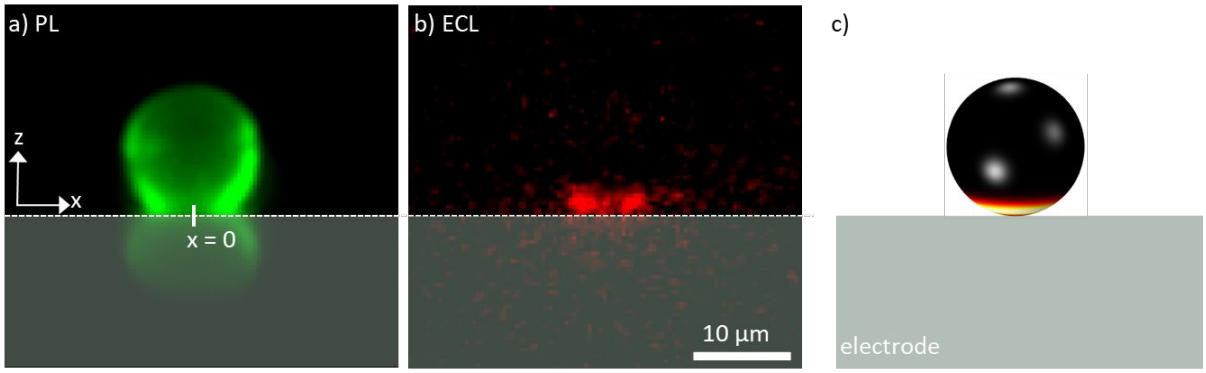

Figure S1. Experimental a) PL and b) ECL images of a single 12-µm diameter Ru@bead deposited on the electrode surface and recorded in the side-view configuration. c) Side-view of the simulated distribution of the ECL intensity (i.e. $[Ru(bpy)_3]^{2+*}$ excited state) considering only the ECL mechanism. The hatched zone represents the luminescence reflection of the Ru@bead on the electrode surface. ECL images were recorded in PBS solution containing 180 mM TPA when imposing a potential of 1.4 V vs Ag/AgCl at the GC electrodes.

2. COMSOL simulation details and parameters of the ECL mechanism

The reactions simulated here were fully described in the main text (see Figure 1d). The heterogeneous electron-transfer reactions and, since those occur at the electrode surface, were simulated in the boundary (flux electrode section). The reaction with the $[Ru(bpy)_3]^{2+}$ attached to the beads were simulate in the surface reaction section. Otherwise, chemical reactions are considered in the subdomain settings. Dependent variables are TPA (named A in the simulation), TPA° (named E in the simulation), TPA°$^{+}$ (named I in the simulation), HTPA (named C in the simulation), other products (named X in the simulation), H^+ (named H in the simulation) for the transport diluted species section and $[Ru(bpy)_3]^{2+}$ (named G in the simulation), $[Ru(bpy)_3]^{+}$ (named G1 in the simulation), $[Ru(bpy)_3]^{2+*}$ (named F in the simulation), and photons (named s_L in the simulation). In order to improve the mesh quality, we also divided the bulk subdomain in two part one close to the electrode (before "z") and another one far from the electrode (after "z"). Those two different subdomains allow to have a precise resolution without a very time-consuming calculation.

Simulation details are described below

2.1 Global Definition

Table S1. Global definition: Simulation parameters

Name	Expression	Value	Description
alpha	0.5	0.5	Electron transfer coefficient
F	96485	96485	Faraday constant [C mol-1]
R	8.314	8.314	Gas constant [J mol-1 K-1]
T	298.15	298.15	Temperature [K]
fa	38.92	38.92	F/RT [V-1]
E0	0.9	0.9	Forward TPA oxidation
D	5e-6[cm^2/s]	5E−10 m^2/s	Diffusion coefficient for TPA
DH	5e-5[cm^2/s]	5E−9 m^2/s	Diffusion coefficient for H
k0	0.01[cm/s]	1E−4 m/s	Heterogeneous ET const [ms-1]
n	1	1	n° of electrons exchanged

Name	Expression	Value	Description
Ea	1.2	1.2	Anodic switching potential [V] (Notice this number may change depending from the switching potential choosed in the simulation)
k3_	3.5e3[1/s]	3500 1/s	Forward constant for deprotonation of RCtpa
k3	1e6[1/(s*M)]	1000 $m^3/(s·mol)$	Backward constant for deprotonation of RCtpa
k1	1e7[1/(s*M)]	10000 $m^3/(s·mol)$	pka of Ctpa
k1_	8e-3[1/s]	0.008 1/s	pkb of TPA
H0	1e-7[M]	1E−4 mol/m^3	ph 7
E0d	-1.7	−1.7	Standard potential for TPA radical oxidation
k5	1e6[1/M/s]	1000 $m^3/(s·mol)$	
k_5	1e-3	0.001	
kem	1e8[1/s]	1E8 1/s	Constant for emission
DRu	5e-10[cm^2/s]	5E−14 m^2/s	
C0	0	0	
Dmin	1e-50	1E−50	
dC	0.000001	1E−6	
A0t	0.180[M]	180 mol/m^3	Initial concentration of TPA
Ru0	1e-3 mol/m^2	1e-3 mol/m^2	Initial concentration of Ru
K	k1/k1_	1.25E6 m^3/mol	
CC0	A0t/(1 + 1/(K*H0))	178.57 mol/m^3	
A0	A0t - CC0	1.4286 mol/m^3	
Rb	6[um]	6E−6 m	Bead radius (Notice this number may change depending from the beads radius in this manuscript we used 1.4 μm or 6 μm)

Table S2. Global definition: Variables

Name	Expression	Unit	Description
kI	k0*exp(-alpha*fa*(Ea - E0))	m/s	Forward constant for TPA oxidation
kA	k0*exp((1 - alpha)*fa*(Ea - E0))	m/s	Backward constant for TPA oxidation
kX	k0*exp(-alpha*fa*(Ea - E0d))	m/s	Forward constant for TPA radical oxidation
kE	k0*exp((1 - alpha)*fa*(Ea - E0d))	m/s	Backward constant for TPA radical oxidation

2.2 Model

Table S3. Model, Definitions Variables

Name	Expression	Unit	Description
t1	0.1	s	Pulse width
t2	0.2	s	Pulse width
dt	0.01	s	Resolution time
f1	flc2hs(t - t1, dt)		Function used for change the potential in the time
f2	flc2hs(t - t2, dt)		Function used for change the potential in the time
r_k1	(-k1*A*H0 + k1_*C)	mol/(m^3·s)	Reaction
r_k3	(k3_*I - k3*E*H0)	mol/(m^3·s)	Reaction
fs_E	k5*s_G*E	mol/(m^2·s)	Flux on beads
fs_I	k5*s_G1*I	mol/(m^2·s)	Flux on beads
r_G	(-fs_E+kem2*s_L)	mol/(m^2·s)	Reaction on beads
r_G1	(-fs_I + fs_E)	mol/(m^2·s)	Reaction on beads
r_L	(-kem2*s_L + fs_I)	mol/(m^2·s)	Reaction on beads
r_F	(+kem2*s_L)	mol/(m^2·s)	Reaction on beads
kem2	kem*1	1/s	
fe_A	(-kA*A + kI*I)	mol/(m^2·s)	Flux on electrode
fe_E	(-kE*E*(E>=0))	mol/(m^2·s)	Flux on electrode
fe_I	(-kI*I + kA*A)	mol/(m^2·s)	Flux on electrode
fe_X	(kE*E*(E>=0))	mol/(m^2·s)	Flux on electrode
r_kd	k1*I*E*(E>=0)	mol/(m^3·s)	

2.3 Geometry

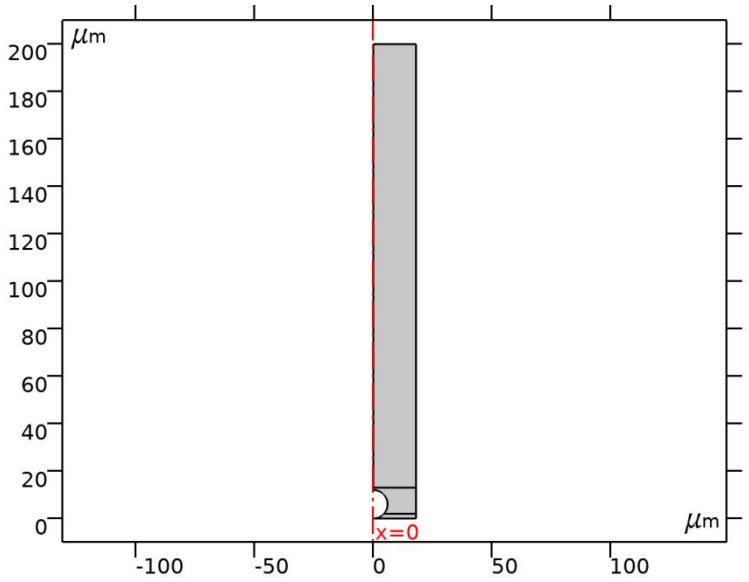

Figure S2. Model geometry. The model geometry used for the simulation is reported in the figure.

2.4 Transport of diluted species

Under transport diluted species: Diffusion, Axial Symmetry, No flux, Initial values, Reaction, Bulk, Flux electrode, Flux beads

Table S4. Diffusion domain 1-3

Description	Value
Diffusion coefficient A	{{D, 0, 0}, {0, D, 0}, {0, 0, D}}
Diffusion coefficient E	{{D, 0, 0}, {0, D, 0}, {0, 0, D}}
Diffusion coefficient I	{{D, 0, 0}, {0, D, 0}, {0, 0, D}}
Diffusion coefficient C	{{D, 0, 0}, {0, D, 0}, {0, 0, D}}
Diffusion coefficient X	{{D, 0, 0}, {0, D, 0}, {0, 0, D}}
Diffusion coefficient H	{{DH, 0, 0}, {0, DH, 0}, {0, 0, DH}}

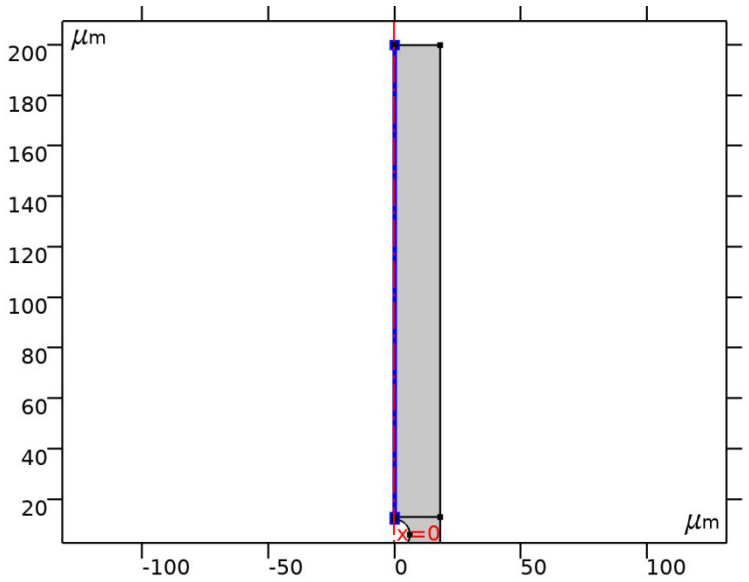

Figure S3. Model Domains: Axial symmetry. Blue line represents the axial symmetry in the model domains.

No flux

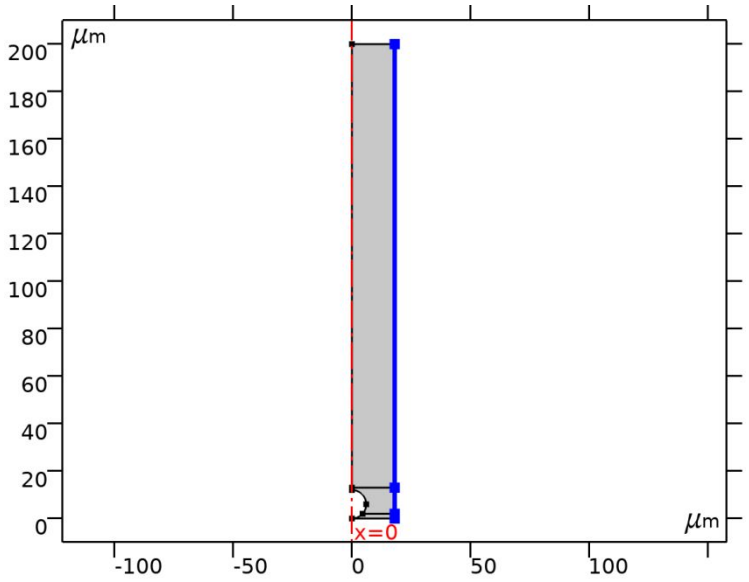

Figure S4. Model Domains: No flux. Blue line is the no flux domain in the model.

Initial values

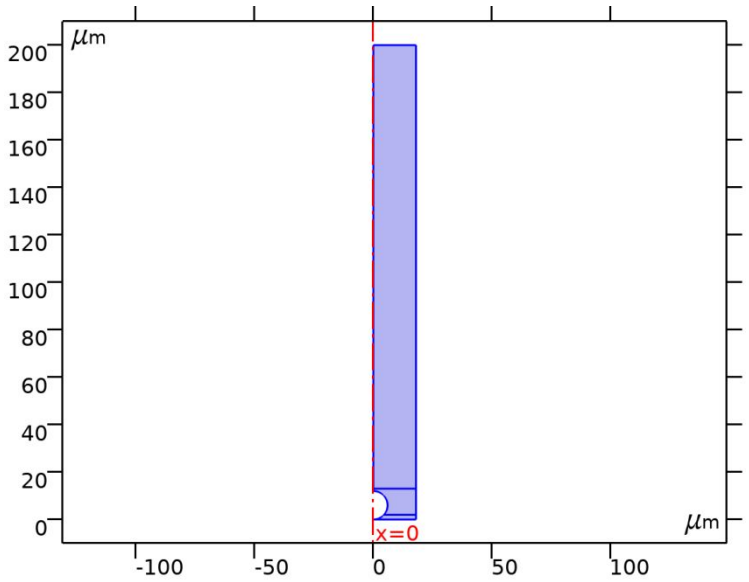

Description	Value
Concentration	{A0, C0, C0, CC0, C0, H0}

Figure S5. Model Domains: Initial values. Blue area is the model domains where initial values are defined.

Reaction

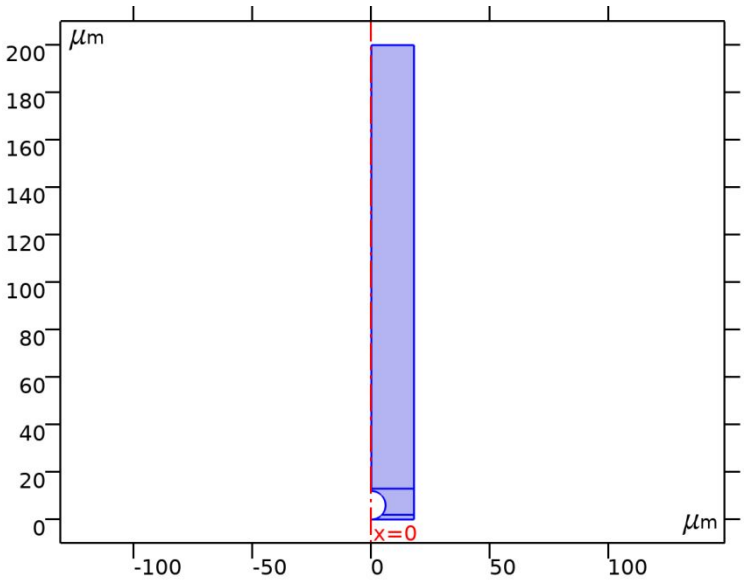

Description	Value
Total rate expression A	r_k1 + r_kd
Total rate expression E	r_k3 - r_kd
Total rate expression I	-r_k3 - r_kd
Total rate expression C	-r_k1
Total rate expression X	r_kd
Total rate expression H	(r_k1 + r_k3)*0

Figure S6. Model Domains: reactions. Blue area is the model domains where the chemical reactions are defined.

Bulk

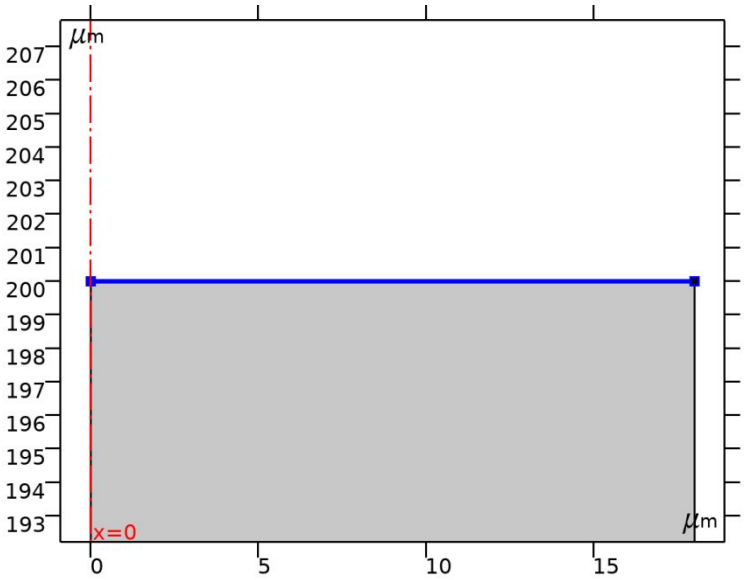

Description	Value
Species A	A0t - C
Species E	C0
Species I	C0
Species C	(A0t)/(1 + 1/(K*H0))
Species X	C0
Species H	H0
Concentration	{A0t - C, C0, C0, (A0t)/(1 + 1/(K*H0)), C0, H0}

Figure S7. Model Domains: Bulk. Blue line is the bulk of the solution in the model domains.

Flux electrode

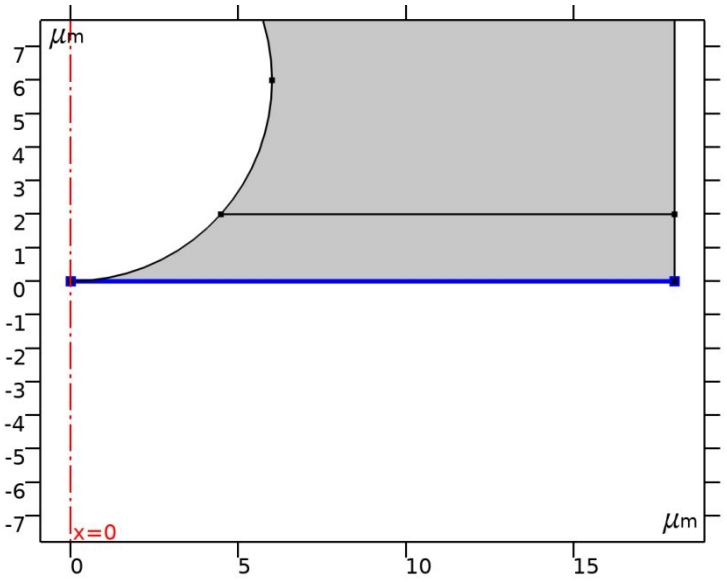

Description	Value
Flux type	General inward flux
Species A	fe_A
Species E	fe_E
Species I	fe_I
Species C	0
Species X	fe_X
Species H	0
	{fe_A, fe_E, fe_I, 0, fe_X, 0}

Figure S8. Model Domains: flux electrode. Blue line is the electrode surface where electrochemical reactions occur in the model.

Flux beads

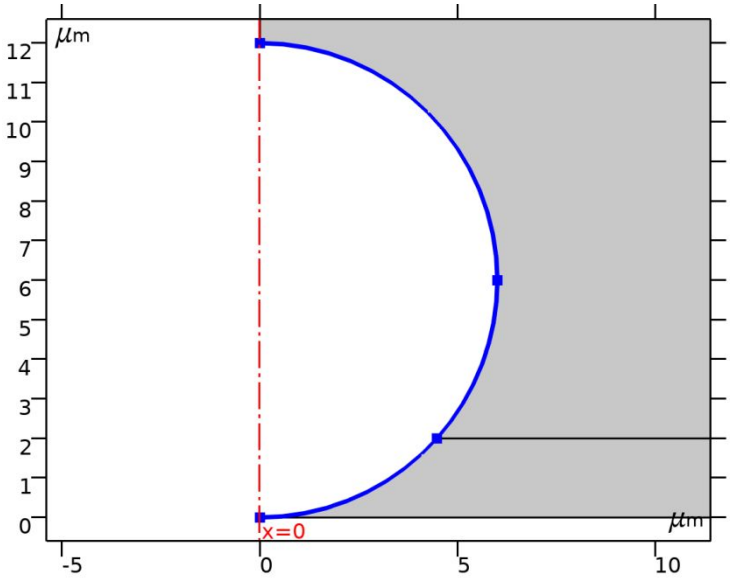

Description	Value
Flux type	General inward flux
Species A	fs_I
Species E	-fs_E
Species I	-fs_I
Species C	0
Species X	fs_E
Species H	0
	{fs_I, -fs_E, -fs_I, 0, fs_E, 0}

Figure S9. Model Domains: flux beads. Blue line is the beads surface.

2.5 Surfaces reactions

Under surface reaction: Surface proprieties, Axial Symmetry, No flux, Initial values, Reaction

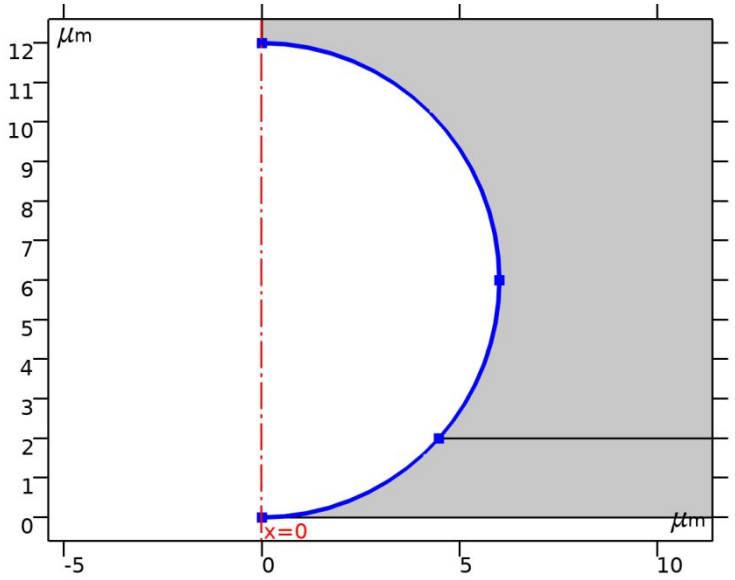

Description	Value
Density of sites	2e-5[mol/m^2]
Site occupancy number	{1, 1, 1, 1}

Description	Value
Surface material	None
Diffusion coefficient G	{{Dmin, 0, 0}, {0, Dmin, 0}, {0, 0, Dmin}}
Diffusion coefficient G1	{{Dmin, 0, 0}, {0, Dmin, 0}, {0, 0, Dmin}}
Diffusion coefficient F	{{Dmin, 0, 0}, {0, Dmin, 0}, {0, 0, Dmin}}
Diffusion coefficient L	{{Dmin, 0, 0}, {0, Dmin, 0}, {0, 0, Dmin}}

Figure S10. Surfaces reactions. Blue line is the beads surface where the luminophore is bound.

Axial Symmetry

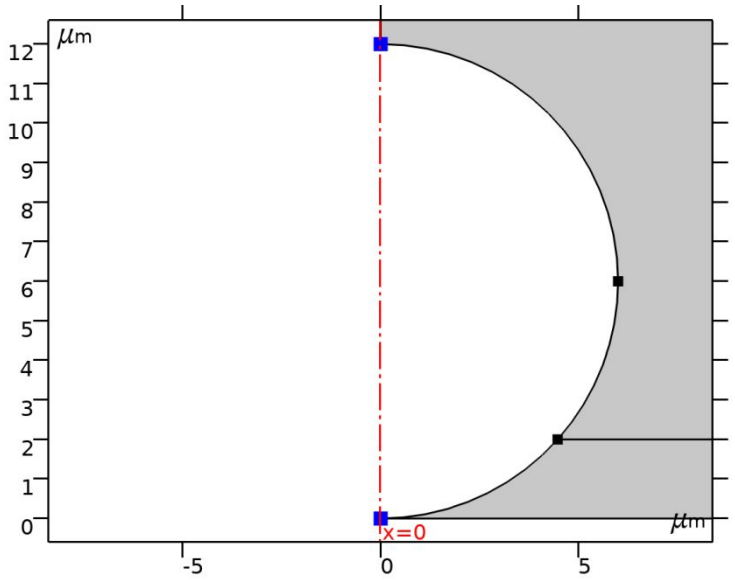

Figure S11. Surfaces reactions: axial symmetry. Blue points are axial symmetry.

No flux

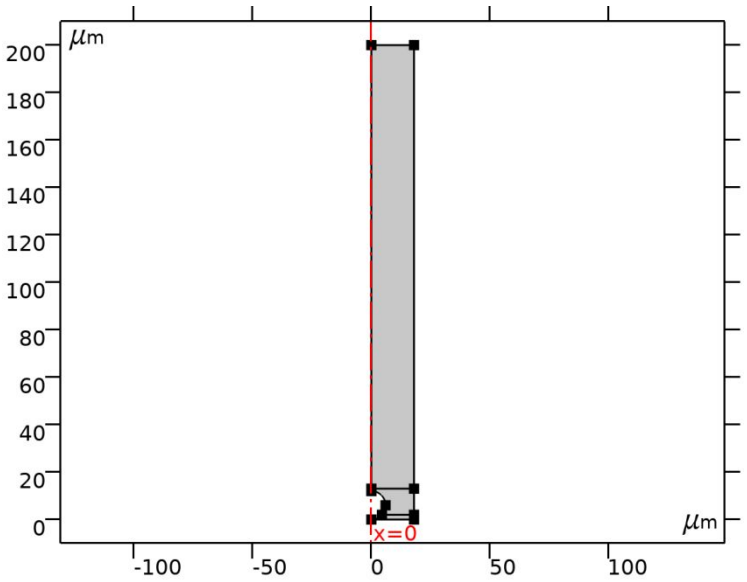

Figure S12. Surfaces reactions: No flux.

Initial values

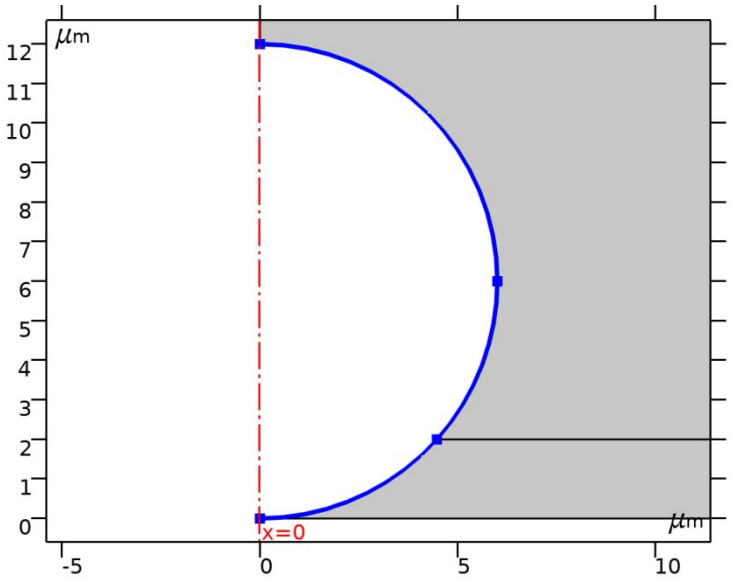

Description	Value
Surface concentration	{1e-3, 0, 0, 0}

Figure S13. Surfaces reactions: Initial value.

Reaction

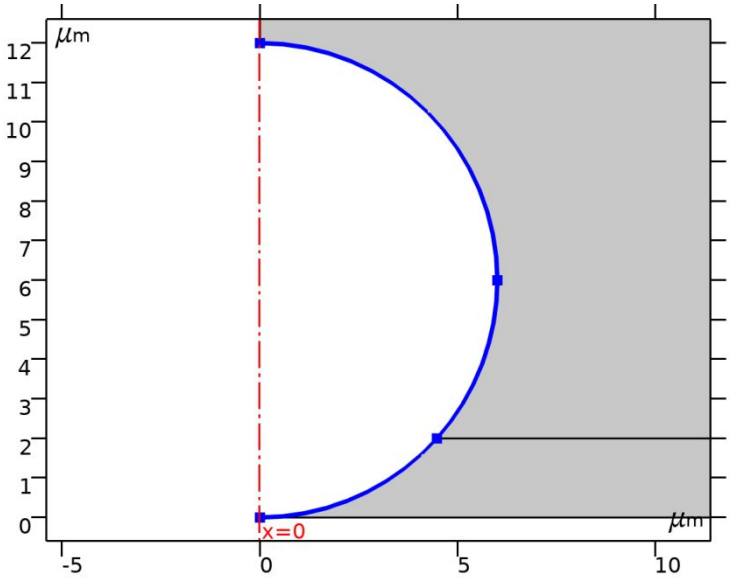

Description	Value
Reaction rate for surface species G	r_G
Reaction rate for surface species G1	r_G1

Description	Value
Reaction rate for surface species F	r_F
Reaction rate for surface species L	r_L

Figure S14. Surfaces reactions: Reactions. Blue line is the beads surface where the luminophore reactions occur.

2.6 Mesh

Size: All the mesh size are reported in μm

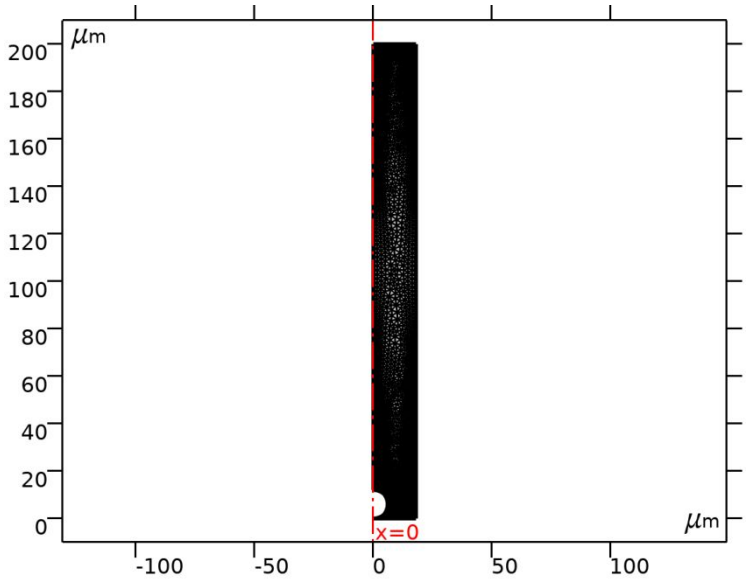

Description	Value
Maximum element size	15
Minimum element size	0.03
Curvature factor	0.3
Maximum element growth rate	1.2
Custom element size	Custom

Figure S15. Model mesh: mesh size.

Free triangular edge:

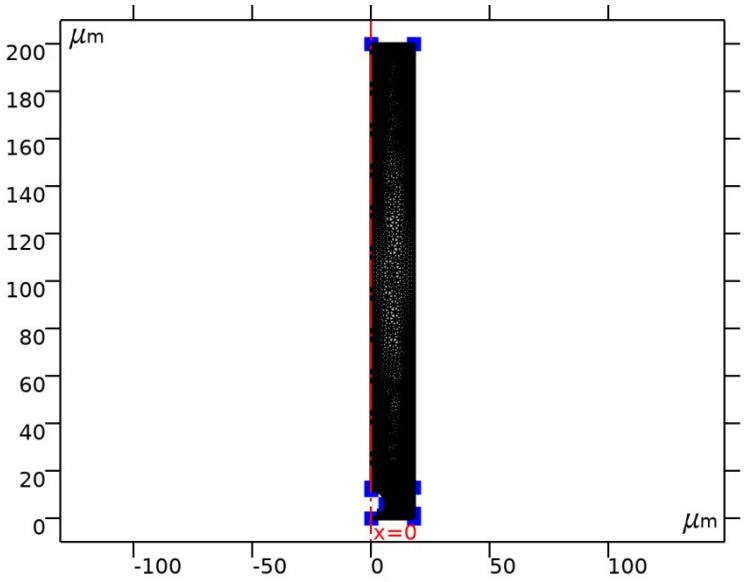

Description	Value
Maximum element size	0.05
Minimum element size	0.0012
Minimum element size	Off
Curvature factor	0.3
Curvature factor	Off
Resolution of narrow regions	Off
Maximum element growth rate	1.02
Custom element size	Custom

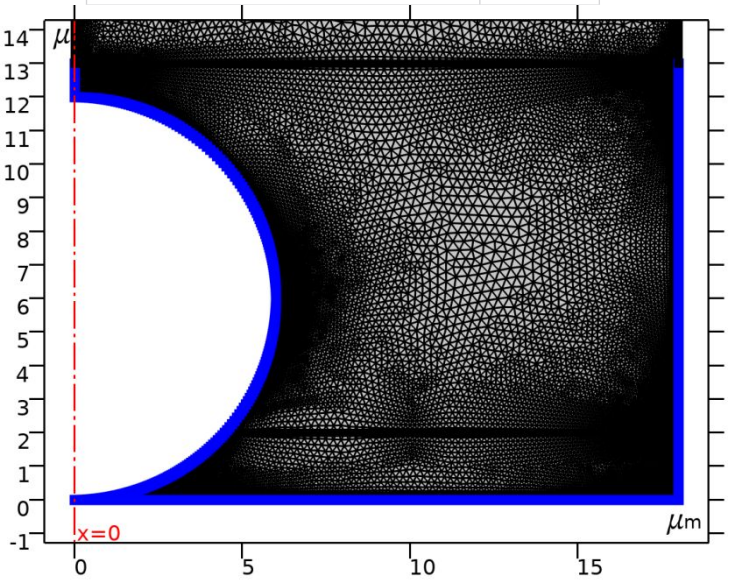

Description	Value
Maximum element size	0.268
Maximum element size	Off
Minimum element size	0.01
Curvature factor	0.3
Curvature factor	Off
Resolution of narrow regions	Off
Maximum element growth rate	1.05
Custom element size	Custom

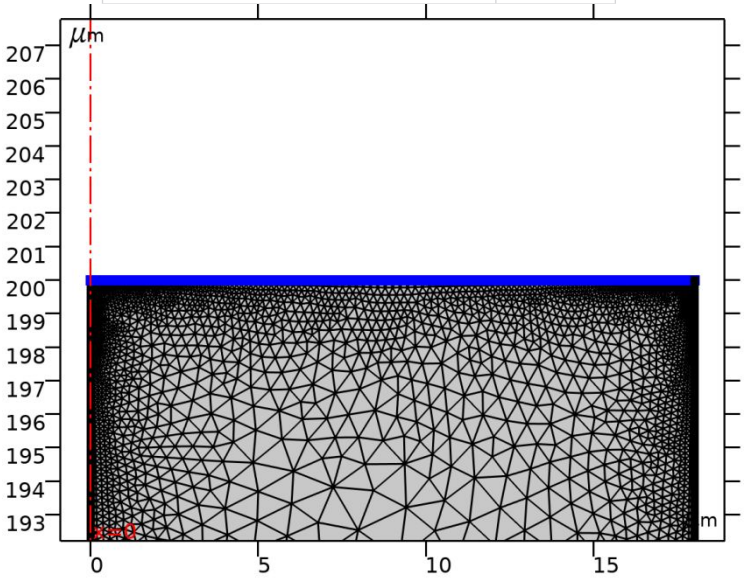

Description	Value
Maximum element size	6.7
Maximum element size	Off
Minimum element size	0.03
Minimum element size	Off
Curvature factor	0.3
Curvature factor	Off
Resolution of narrow regions	Off
Maximum element growth rate	1.05
Custom element size	Custom

Figure S16. Model mesh: Free triangular.

Boundary layers:

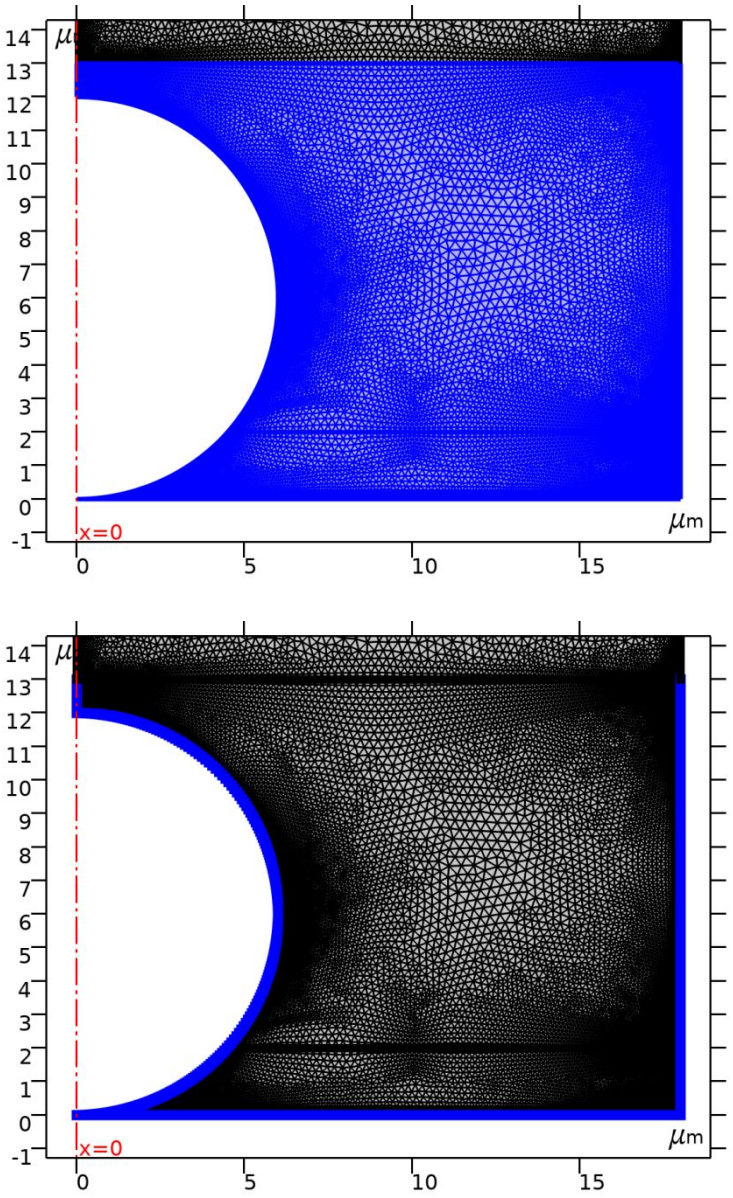

Description	Value
Number of boundary layers	10
Boundary layer stretching factor	1.02
Thickness of first layer	Manual
Thickness	0.02

Figure S17. Model mesh: Boundary layers.

2.7 Study

Table S5. Time dependent solver

Times	Unit
0 10^{range(-7,1,-2)} range(0.05,0.05,1)	s

Description	Value
Times	{0, 1.0E-7, 1.0E-6, 1.0E-5, 1.0E-4, 0.001, 0.01, 0.05, 0.1, 0.15000000000000002, 0.2, 0.25, 0.3, 0.35000000000000003, 0.4, 0.45, 0.5, 0.55, 0.6000000000000001, 0.6500000000000001, 0.7000000000000001, 0.7500000000000001, 0.8, 0.8500000000000001, 0.9000000000000001, 0.9500000000000001, 1}
Tolerance	User controlled
Relative tolerance	0.1

3. Comparison of the simulated ECL images

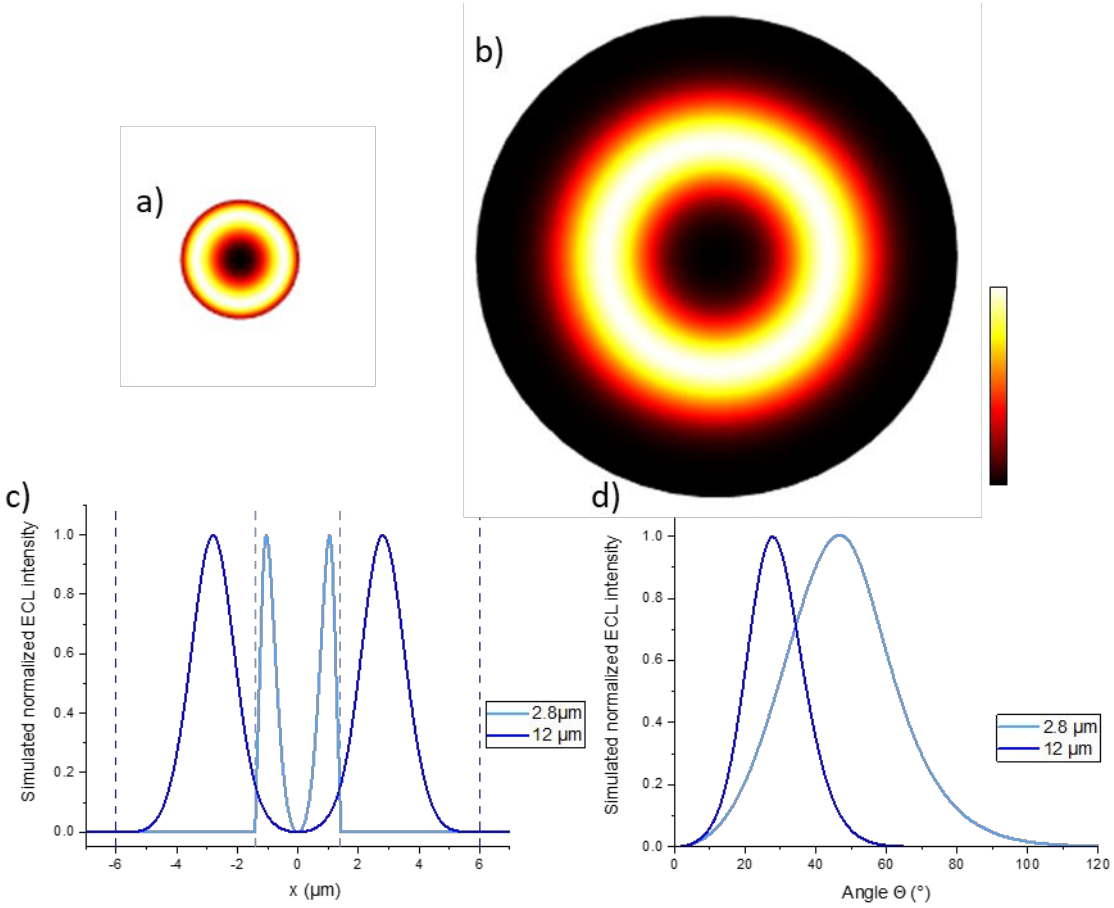

Figure S18. Comparison of the simulated ECL images of a single a) 2.8-µm and b) a 12-µm diameter Ru@bead considering only the ECL mechanism. Corresponding c) ECL intensity profiles and d) angular dependence $\rho(\theta)$ of the ECL signal for both Ru@beads.

4. (Top) Simulated ECL images 12-µm diameter Ru@bead

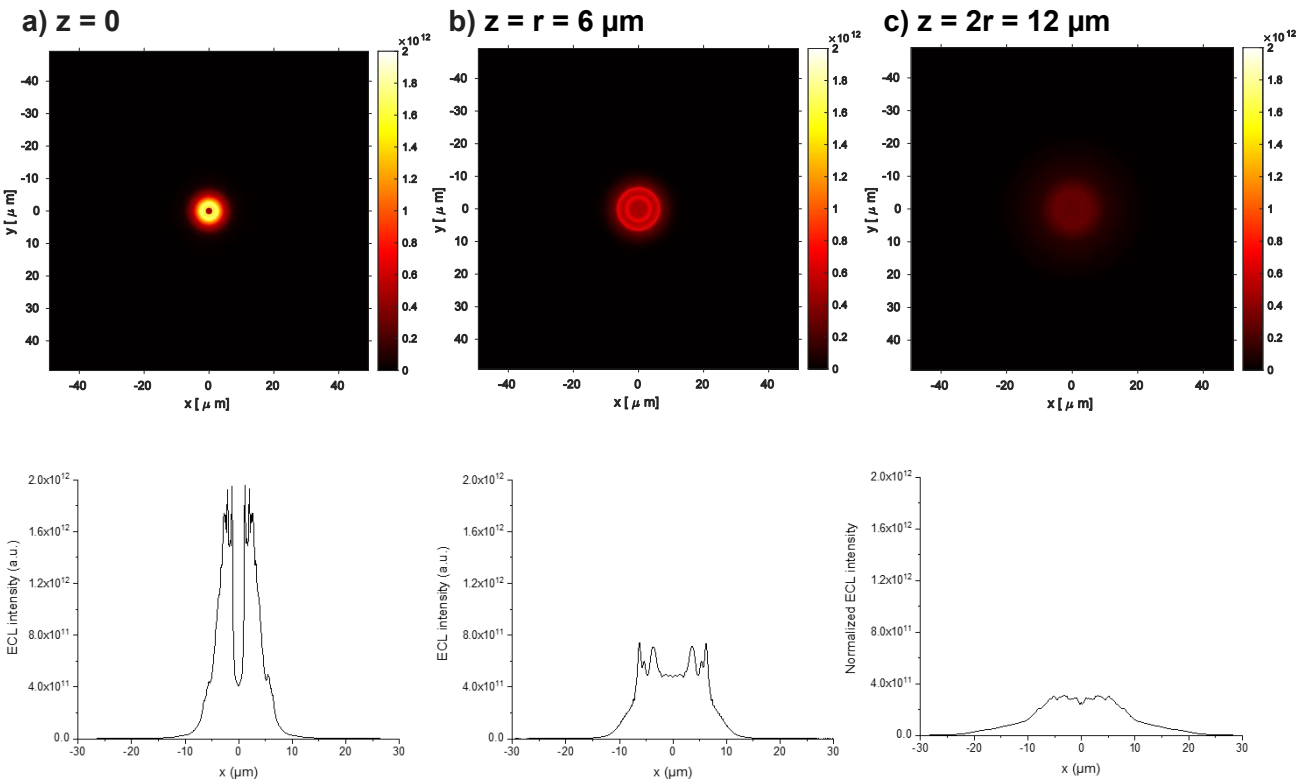

Figure S19. (Top) Simulated ECL images of a single 12-µm diameter Ru@bead deposited on the electrode surface in the top-view configuration with different focal planes: a) bottom (z =0), b) middle (z = 6 µm) and c) top (z = 12 µm). (Bottom) Corresponding ECL intensity profiles for different *z* values. The images were simulated considering the ECL mechanism and the optical effects.

5. (Top) Simulated ECL images of a single 2.8-µm diameter Ru@bead

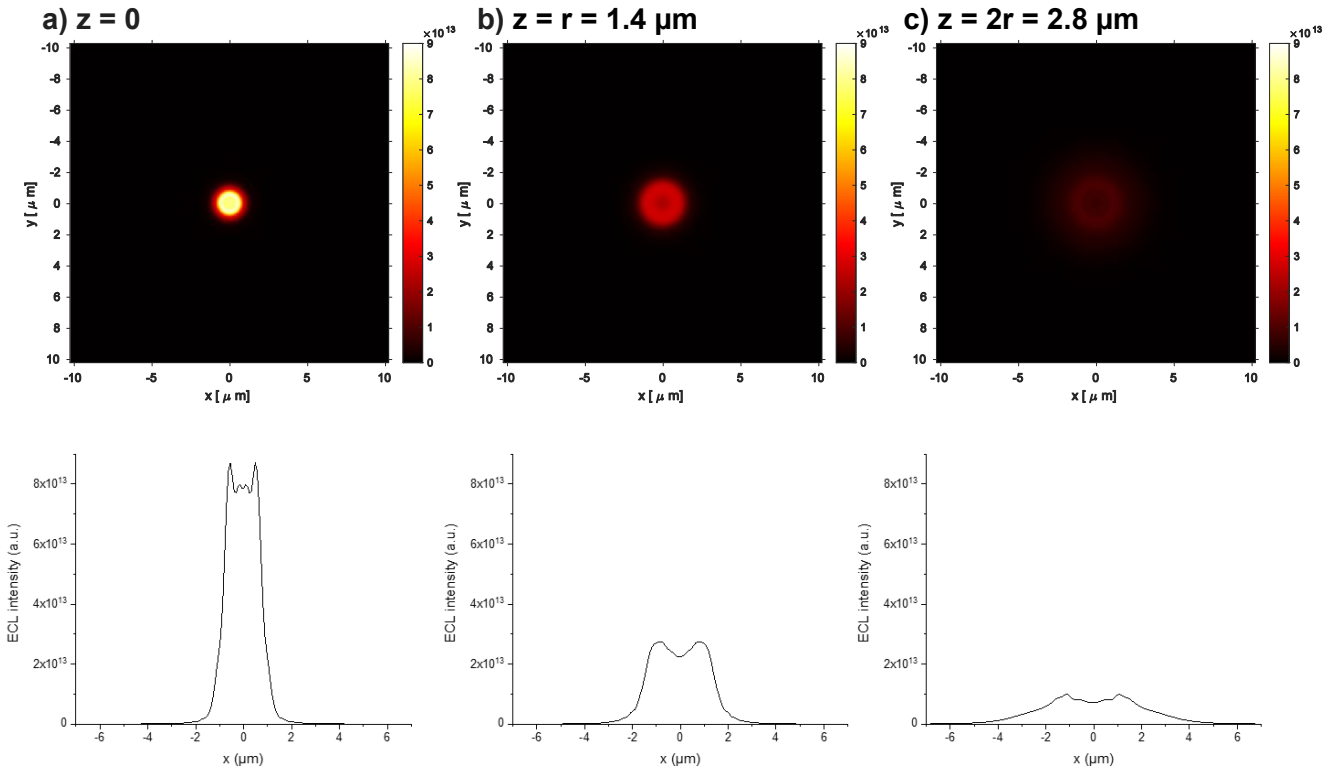

Figure S20. (Top) Simulated ECL images of a single 2.8-µm diameter Ru@bead deposited on the electrode surface in the top-view configuration with different focal planes: a) bottom (z =0), b) middle (z = 1.4 µm) and c) top (z = 6 µm). (Bottom) Corresponding ECL intensity profiles for different *z* values. The images were simulated considering the ECL mechanism and the optical effects.

6. Experimental Section

Reagents. All the reagents were purchased from Sigma-Aldrich unless otherwise noted. PS beads were obtained from Kisker Biotech GmbH & Co. Phosphate buffer solution (pH 7.4, 0.1 M) was prepared by mixing 0.1 M sodium phosphate monobasic monohydrate and 0.1 M sodium phosphate dibasic heptahydrate solution with degassed solution. TPA was dissolved in PBS and the pH was adjusted to 7.4 with phosphoric acid. Capture antibody specific for interleukin 8 (IL-8), the complementary biotinylated detection antibody and IL-8 recombinant protein were obtained from R&D Systems Inc.

Functionalization of the PS beads. The functionalization of the beads by the ECL labels using both immunoassay and peptidic approaches has been described previously.[1-3] In the first case, antigen storage aliquots were prepared in PBS 1x/BSA 0.1% and detection antibody storage aliquots were prepared in tris-buffered saline (TBS StartingBlock). Each washing step was done in 100 µL of TBS with 1% Tween 20. The assay was performed by incubating for 2 h the microbeads functionalized with a capture antibody (anti-IL-8) first in a sample containing antigen (dilute to the appropriate concentration with PBS Starting Block) and washed. Then they were incubated for 30 min in 50 µL of the biotinylated detection antibodies solution (3 µg/mL of antibody in PBS StartingBlock) and washed. Finally, the ECL label was attached to form immunocomplex by exposing the beads to a solution containing a streptavidin-modified $[Ru(bpy)_3]^{2+}$ label. In the second case, the surface of the PS beads beared $-NH_2$ groups which allow further functionalization with the ECL $[Ru(bpy)_3]^{2+}$ label. 10 µL of beads suspension (2.5%) was washed with PBS (pH 7.4) and re-suspended in 1 mL of PBS. In the same time, 1 mg of $[Ru(bpy)_3]^{2+}$-NHS ester (bis(2,2′-bipyridine)-4′-methyl-4-carboxybipyridine-ruthenium N-succinimidyl ester-bis(hexafluorophosphate) was dissolved in 100 µL of dimethyl sulfoxide and this solution was added to the bead suspension. This mixture was incubated on +4 °C for 3 h with continuous stirring. After the incubation the beads were washed from reaction solution with PBS 10 times by the centrifugation for 10 min at 10,000 rpm to separate the beads from the solution. Finally, beads were suspended in 1 mL PBS and kept at 4 °C.

Instrumentation. The electrochemical cell was a 3-electrode system where the working electrode was glassy carbon (GC). A platinum wire was used as the counter electrode and Ag/AgCl/KCl (3 M) electrode was used as the reference electrode. The experiments were performed using a µ-Autolab type Ⅲ potentiostat. The PL and ECL images were recorded using an epifluorescence

microscope from Leica (DMI6000, Leica Microsystems) and an Electron Multiplying Charge Coupled Device (EM-CCD 9100–13) Camera from Hamamatsu. The working electrode was placed in two different configurations inside the electrochemical cell for top-view and side–view study.

7. References

(1) Deiss, F.; LaFratta, C. N.; Symer, M.; Blicharz, T. M.; Sojic, N.; Walt, D. R. Multiplexed Sandwich Immunoassays using Electrochemiluminescence Imaging Resolved at the Single Bead Level. *J. Am. Chem. Soc.* **2009**, *131*, 6088-6089.
(2) Sentic, M.; Milutinovic, M.; Kanoufi, F.; Manojlovic, D.; Arbault, S.; Sojic, N. Mapping electrogenerated chemiluminescence reactivity in space: mechanistic insight into model systems used in immunoassays. *Chem. Sci.* **2014**, *5*, 2568-2572.
(3) Dutta, P.; Han, D.; Goudeau, B.; Jiang, D.; Fang, D.; Sojic, N. Reactivity mapping of luminescence in space: Insights into heterogeneous electrochemiluminescence bioassays. *Biosens. Bioelectron.* **2020**, *165*, 112372.